

Sub-nanosecond silicon-on-insulator optical micro-ring switch with low crosstalk

Xi Xiao (肖希)*, Haihua Xu (徐海华), Liang Zhou (周亮), Zhiyong Li (李智勇),
Yuntao Li (李运涛), Yude Yu (俞育德), and Jinzhong Yu (余金中)

State Key Laboratory on Integrated Optoelectronics, Institute of Semiconductors,
Chinese Academy of Sciences, Beijing 100083, China

*E-mail: xixiao@semi.ac.cn

Received March 3, 2010

We demonstrate a sub-nanosecond electro-optical switch with low crosstalk in a silicon-on-insulator (SOI) dual-coupled micro-ring embedded with p-i-n diodes. A crosstalk of -23 dB is obtained in the $20\text{-}\mu\text{m}$ -radius micro-ring with the well-designing asymmetric dual-coupling structure. By optimizations of the doping profiles and the fabrication processes, the sub-nanosecond switch-on/off time of < 400 ps is finally realized under an electrical pre-emphasized driving signal. This compact and fast-response micro-ring switch, which can be fabricated by complementary metal oxide semiconductor (CMOS) compatible technologies, have enormous potential in optical interconnects of multicore networks-on-chip.

OCIS codes: 130.3120, 250.6715, 230.5750, 230.4000.

doi: 10.3788/COL20100808.0757.

The rapid development of silicon photonics, including modulators, switches, and Ge-on-Si photodetectors, has indicated the feasibility of on-chip optical interconnects in multicore computing systems. Significant increments of computation performance can be expected if high-data-rate optical signals can be switched with low power. A silicon-based micro-resonator has been considered as the key component for the optical networks-on-chip for its compactness, wavelength selectivity, and low power consumption^[1–4]. Some studies on silicon micro-resonator-based optical switches have been reported, aiming at on-chip multiplexing/demultiplexing and routing of wavelength division multiplexing signals with low power and large bandwidth^[5–9]. However, most of the reported crosstalks and switch times are not sufficient for future fast on-chip optical switching with transmission bit rates exceeding 10 Gb/s. A compact and low crosstalk silicon-based electro-optical switch operating in the sub-nanosecond regime remains to be demonstrated for on-chip optical interconnects.

In this letter, we demonstrate a 1×2 silicon-on-insulator (SOI) based micro-ring switch with low crosstalk and sub-nanosecond switch time. The switch crosstalk of -23 dB is obtained with the optimized asymmetric dual-coupling micro-ring. Through the lateral p-i-n diodes integrated to the ring waveguide, carrier-induced plasma dispersion effect^[10] is utilized to fast-switch the resonance of the micro-ring. An electrical pre-emphasized driving signal is generated and employed for switch speed acceleration. A sub-nanosecond switch-on/off time of 300/380 ps is realized.

The switch consists of a $20\text{-}\mu\text{m}$ -radius dual-coupling micro-ring surrounded by p+ and n+ doped regions. Figure 1(a) is the top-view microscope image of the fabricated switch with Al electrodes. The gray lines highlight the $20\text{-}\mu\text{m}$ -radius micro-ring and the coupling waveguides. Under forward bias, the embedded p-i-n diodes inject the carriers into the intrinsic waveguide. The variation of the carrier density changes the refractive index

and absorption coefficient because of the plasma dispersion effect in silicon^[10]. In this way, the driving electrical signal shifts the micro-ring resonance and controls the on/off state of the optical signals produced from the through- and drop-ports.

Figure 1(b) shows the cross-sectional schematic of the micro-ring waveguide and the integrated lateral p-i-n diodes. The waveguide was fabricated on a SOI wafer with a 340-nm top silicon layer. All the waveguides have ~ 100 nm slab thickness for the electrical integration and are single mode waveguides designed for transverse electric (TE) mode transmission. The operation speed of a forward p-i-n diode is significantly dependent on the carrier transport distance across the waveguide^[11,12];

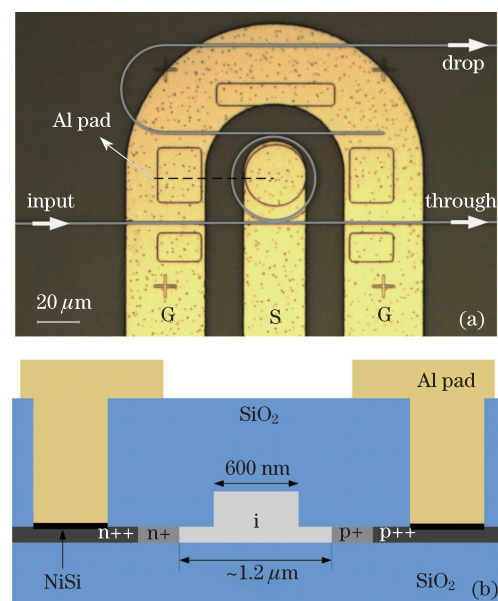


Fig. 1. (a) Top-view microscope image of the micro-ring switch; (b) cross-section schematic of the fabricated ring waveguide integrated with forward p-i-n diodes.

thus, shortening the width of the intrinsic region is an essential way of decreasing the switch time. We located both the p+ and n+ regions 300 nm away from the edges of the ring waveguide using boron and phosphorous implantations with concentrations of $\sim 10^{19} \text{ cm}^{-3}$. Resistance-capacitance time constant was also taken into consideration for sub-nanosecond operations. To obtain good ohmic contacts and low absorption losses, more highly doped regions p++ and n++ with concentrations more than 10^{20} cm^{-3} were implanted with moderate distances from the intrinsic waveguide. A thin nickel-silicide film was later formed by metal evaporation and rapid thermal annealing because the low resistivity of this film improves the metal contact to the highly doped regions.

The optical configuration of the micro-ring directly determines switch characteristics, such as crosstalk and bandwidth. Thus, the waveguide-to-ring coupling strengths were especially designed for moderate quality (Q) factor and low crosstalk. The asymmetric dual-coupling structure, which has different optical coupling efficiencies to the input and the drop waveguides, was adopted for its characteristics of large through-port extinction ratio (ER) and low crosstalk^[13,14]. A high through-port ER and low crosstalk can be obtained when drop-side coupling is appropriately weakened for a critical coupling condition (the through-side waveguide-to-ring coupling matches the sum of waveguide loss per round in the ring and the drop-side ring-to-waveguide coupling)^[15]. Figure 2 shows the passive structure of the asymmetric micro-ring switch in detail. Advanced electron beam lithography and silicon etching processes were employed to accurately control the device dimensions in nanometer-scale tolerance. The measured widths of the bus waveguides and ring waveguide are 400 and 600 nm, respectively. The through- and drop-side gap widths are 220 and 250 nm, respectively. The experimental results agree well with the designed dimensions determined by numerical three-dimensional (3D) simulations using beam propagation method. The optical loss in the micro-ring was carefully suppressed during the fabrications; thus, the slight increment in the gap width of $\sim 30 \text{ nm}$ was suitable for improving the crosstalk between the through-

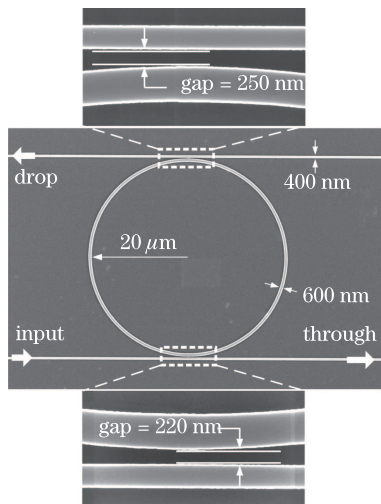


Fig. 2. Scanning electronic microscope (SEM) images of the passive micro-ring switch with the asymmetrical gap widths.

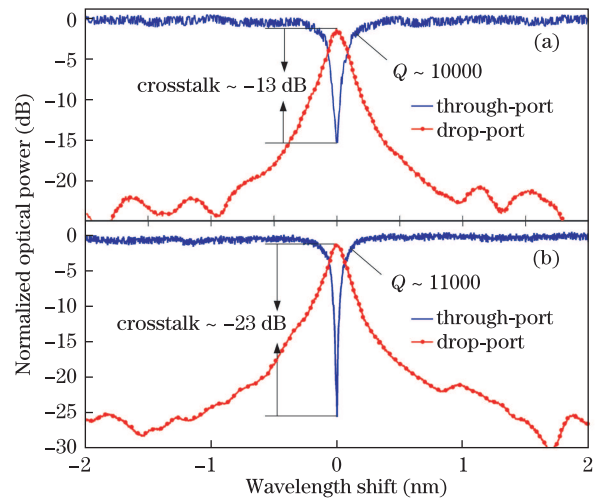


Fig. 3. Transmission spectra of (a) symmetric micro-ring switch and (b) asymmetric micro-ring switch.

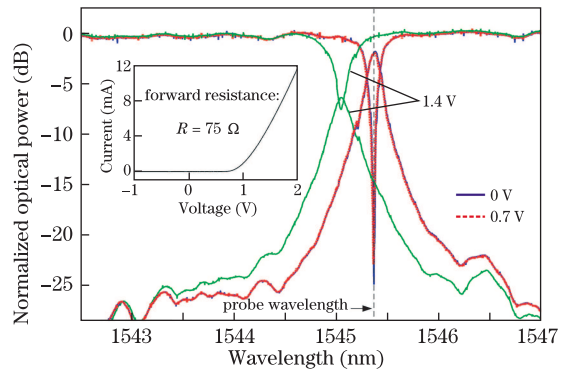


Fig. 4. Transmission spectra of the micro-ring resonator under the bias voltages of 0, 0.7, and 1.4 V. Inset: current-voltage curve of the micro-ring switch.

and drop-ports.

Both the static and dynamic performances of the electro-optic micro-ring switch were characterized. The optical spectrum curves of the asymmetric micro-ring switch are plotted in Fig. 3, and compared with the optical responses of a symmetric micro-ring switch. The two rings were fabricated together on the same wafer and have identical dimensions except for the drop-side gap width. The gap widths of the symmetric micro-ring switch are 220 nm at both sides. The asymmetric micro-ring has asymmetric gaps of 220 and 250 nm, as mentioned above. The through-port ER of the symmetric ring was $\sim 16 \text{ dB}$, while the through-port ER was increased to 25 dB with asymmetric configuration. On account of the highly enhanced through-port ER, the in-band crosstalk of through- and drop-channels was suppressed to $< -23 \text{ dB}$, showing a 10-dB improvement from the symmetric micro-ring. A moderate Q factor of ~ 11000 (bandwidth $\sim 18 \text{ GHz}$) was measured when $\lambda_0 = 1545.4 \text{ nm}$. This Q factor not only enables a high switch speed but also allows high bit rate transmission beyond 10 Gb/s ^[16].

Figure 4 shows the optical transmission spectra before and after a direct current (DC) bias with the inset showing the current-voltage characteristics of the p-i-n diode. The turn-on voltage of the p-i-n diodes is about

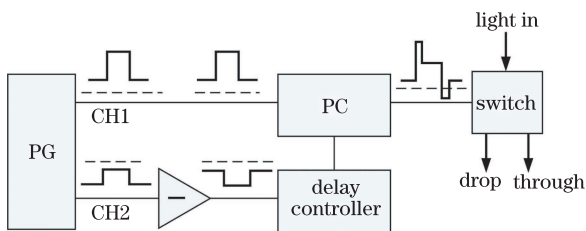


Fig. 5. Schematic of experimental setup for the generation of pre-emphasized driving signals.

0.7 V, which results from the narrow width of the intrinsic region. The forward differential resistance of $\sim 75 \Omega$ indicates good metal contacts. As shown in Fig. 4, when the switch is biased to 0.7 V, the through- and drop-port spectrum curves are almost stable as the little carriers are injected around the turn-on voltage. The resonant wavelength was blue-shifted for $\sim 0.32 \text{ nm}$ while under a 1.4-V forward DC bias. This small resonance shift is sufficient for the optical switching due to the high resonating capability of the micro-ring. High ERs were measured at the through- and drop-ports to be 25 and 13 dB, respectively, while the DC power consumption was only 5.3 mW.

The electrical pre-emphasized signals were adopted to drive the micro-ring switch. We developed a new method to generate the pre-emphasized driving signals by combining two square wave signals. Not only can we determine the voltage levels with this generation method, but also adjust the width of the pre-emphasized pulse. Two channels of electrical square wave signals (CH1 and CH2) with the same wave width and different voltage levels were generated by a pattern generator (PG) (Fig. 5). The electrical square wave signal with low voltage levels (CH2) was inverted and transmitted to a delay controller. The delay controller adjusts the relative temporal locations of these two square waves and actually determines the width of the pre-emphasized pulse. The two output square waves were then combined using an electrical power combiner (PC) and applied to the switch.

Figure 6(a) shows the waveform of the pre-emphasized driving signal with an emphasis pulse width of 500 ps. The switch on and off voltages were 1.4 and 0.7 V, respectively, while the forward and reverse pre-emphasized voltages were 2.5 and -0.5 V , respectively. Figures 6(b) and (c) are the normalized optical power measured from the through- and drop-ports, respectively. The switch-off voltage was set close to the turn-on voltage ($\sim 0.7 \text{ V}$) of the p-i-n diode; thus, the carrier densities (as well as refractive index) in the waveguide immediately changed when the forward pre-emphasized pulse was applied, leading to a short 10% to 90% switch-on time of $\sim 300 \text{ ps}$. When the carrier densities began to stabilize, the driving voltage was decreased to 1.4 V to maintain the switch-on state with the lowest carrier density levels. When the reverse emphasized pulse was applied to the switch, the carriers were swept out of the waveguide under the reverse electric field with little carrier storage time, resulting in a $\sim 380 \text{ ps}$ switch-off time. We attribute the relatively longer switch-on time to the limited voltage level of the reverse pre-emphasized pulse. Higher switching speed is realized if the pre-emphasized

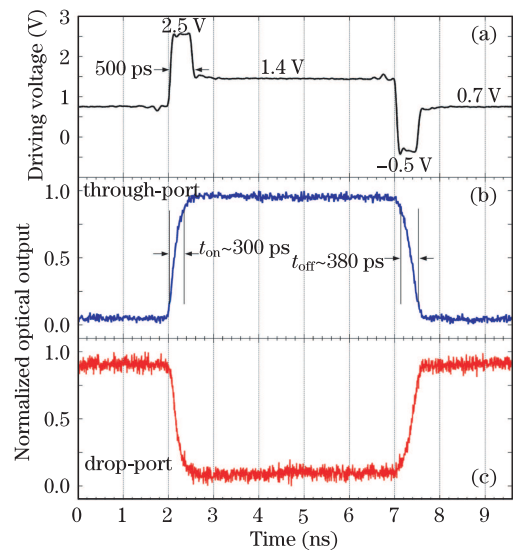


Fig. 6. Dynamic optical responses of the micro-ring switch driven by a pre-emphasized signal. (a) Measured waveform of the pre-emphasized signal; (b) measured optical response at the through-port; (c) measured optical response at the drop-port.

pulse voltages are amplified. However, to the best of our knowledge, these are already the shortest switch times ever demonstrated in silicon-based electro-optical micro-resonator switches^[9].

In conclusion, we fabricate a SOI-based electro-optic switch based on a $20\text{-}\mu\text{m}$ -radius micro-ring and forward p-i-n diodes with complementary metal oxide semiconductor (CMOS) compatible technologies. An asymmetric dual-coupling configuration is adopted and carefully optimized for large ERs and low crosstalk. The through- and drop-port ERs are measured to be 25 and 13 dB in the asymmetric ring, respectively. A low crosstalk of $< -23 \text{ dB}$ is also obtained, showing a 10-dB crosstalk improvement from the symmetric configuration. Advanced silicon fabrication technologies are employed for sub-nanosecond operations, including narrowing the intrinsic region of the p-i-n diode and reducing the conductor resistance. A novel generation method of pre-emphasized driving signals is developed to enhance speed. Finally, a fast-response electro-optical switching is demonstrated with the switch-on/off times of 300/380 ps, respectively.

This work was supported by the State Key Development Program for Basic Research of China (No. 2006CB302803) and the National Natural Science Foundation of China (No. 60877036).

References

1. A. W. Poon, X. Luo, F. Xu, and H. Chen, *Proc. IEEE* **97**, 1216 (2009).
2. A. Shacham, K. Bergman, and L. P. Carloni, in *Proceedings of the 1st IEEE International Symposium on Networks-on-Chips (NOCS 2007)* (2007).
3. B. Timotijevic, G. Mashanovich, A. Michaeli, O. Cohen, V. M. N. Passaro, J. Crnjanski, and G. T. Reed, *Chin. Opt. Lett.* **7**, 291 (2009).
4. Z. Xia, H. Yi, Y. Chen, and Z. Zhou, *Chin. Opt. Lett.* **7**, 598 (2009).

5. M. R. Watts, D. C. Trotter, and R. W. Young, in *Optical Fiber Communication Conference and Exposition and the National Fiber Optic Engineers Conference Technical Digest PDP14* (2008).
6. H. L. R. Lira, S. Manipatruni, and M. Lipson, *Opt. Express* **17**, 22271 (2009).
7. N. Sherwood-Droz, H. Wang, L. Chen, B. G. Lee, A. Biberman, K. Bergman, and M. Lipson, *Opt. Express* **16**, 15915 (2008).
8. Y. Vlasov, W. M. J. Green, and F. Xia, *Nature Photon.* **2**, 242 (2008).
9. X. Luo, S. Feng, and A. W. Poon, in *Proceedings of the 14th Optoelectronics and Communications Conference (OECC 2009) ThG2* (2009).
10. R. A. Soref and B. R. Bennett, *IEEE J. Quantum Electron.* **23**, 123 (1987).
11. X. J. Xu, S.-W. Chen, H.-H. Xu, Y. Sun, Y.-D. Yu, J.-Z. Yu, and Q.-M. Wang, *Chin. Phys. B* **18**, 3900 (2009).
12. C. E. Png, S. P. Chan, S. T. Lim, and G. T. Reed, *J. Lightwave Technol.* **22**, 1573 (2004).
13. A. Vörckel, M. Mönster, W. Henschel, P. H. Bolivar, and H. Kurz, *IEEE Photon. Technol. Lett.* **15**, 921 (2003).
14. P. Dong, S. F. Preble, and M. Lipson, *Opt. Express* **15**, 9600 (2007).
15. A. Yariv, *Electron. Lett.* **36**, 321 (2000).
16. Q. Xu, B. Schmidt, J. Shakya, and M. Lipson, *Opt. Express* **14**, 9430 (2006).